IJCRT.ORG ISSN : 2320-2882

INTERNATIONAL JOURNAL OF CREATIVE RESEARCH THOUGHTS (IJCRT)

An International Open Access, Peer-reviewed, Refereed Journal

FLUORESCENCE ENHANCEMENT OF CHALCONE DERIVATIVES BY SEMICONDUCTOR NANOPARTICLES

[1] Nirupama J.M, [2] Rajesh. G. Kalkhambkar, [3] Shruti. S. Malunavar, [4]V. Praveenkumar, [5]G.H.Malimath

[1]Assistant Professor, [2]Assistant Professor, [3]Research Scholar, [4]Research Scholar, [5]Professor

[1, 4, 5] Department of Physics, [2,3]Department of Chemistry,

[1,2,3,4,5] Karnatak Science College, Dharwad, India

Abstract: Interaction of substituted chalcone derivatives, 4-phenylbut-3-en-2-one, (E)-3-(4-hydroxyphenyl)-1-phenylprop-2-en-1-one and 3-(2-hydroxyphenyl)-1-phenylprop-2-en-1-one with the semiconductor nanoparticles such as TiO_2 and ZnO were studied by UV-VIS absorption, fluorescence spectroscopy, FT-IR, and Cyclic Voltammetry. The Global chemical reactivity descriptor (GCRD) parameters, HOMO, LUMO, energy gap, and Molecular electrostatic potential (MESP) plots were obtained for the chalcone derivatives using DFT, B3LYP level, 6-311G basis set in Gaussian 09W. Benesi-Hildebrand plots were used to understand the stoichiometric interactions between chalcone derivative and semiconductor nanoparticles. All three chalcone derivatives exhibit fluorescence enhancement in the presence of semiconductor nanoparticles. Chalcone derivative, 3-(2-hydroxyphenyl)-1-phenylprop-2-en-1-one shows the selective response to TiO_2 and ZnO in acetonitrile solvent. The energy gap value determined from Cyclic Voltammogram is very close to the value obtained from the DFT computation. From the spectroscopic and DFT computational study, these chalcone derivatives have potential applications in nonlinear optics.

Index Terms **- fluorescence enhancement; chalcone derivative; energy gap; chemical reactivity; computation**

1.INTRODUCTION

Chalcone derivatives are known for their antimicrobial, antitumor, anti-HIV, anti-malarial, anti-inflammatory, and anti-carcinogenic activities. Apart from their wide application in the fields of biology and medicine, they are also exploited in photorefractive polymers, holographic recording materials, and also as fluorescent sensors for detecting toxic metal ions [1]. Bromo and methyl-substituted chalcone derivatives are preferred in nonlinear optics (NLO) compared to inorganic molecules because they are easy to synthesize, damage resistant, and ultrafast in response [2]. The global chemical reactivity descriptor parameters determined from the DFT study indicate that 1,3-diphenyl-2-propen-1-one chalcone and its derivatives are stable and hence these derivatives have application in nonlinear optical materials [3]. The chalcone's aggregation-induced enhanced emission (AIEE) property with Donor-π-Acceptor architecture has numerous optoelectronic applications. Chalcone derivatives with electron-donating functional groups increased the emissive efficiency. As hydrogen can be easily replaced in chalcone derivatives, they are used to design optical sensors, solar cells, and liquid crystals [4]. Chalcone derivatives are preferred in photo initiation systems (PIS) because they absorb light in the uv-vis region [5]. The Chalcone derivative, KCP, is a very sensitive and selective fluorescent probe for detecting highly toxic thiophenol. KCP exhibits 160-fold fluorescence enhancement and a large Stokes shift of 130 nm in the presence of thiophenol [6]. The excess consumption of aluminium may be responsible for Parkinson's and Alzheimer's diseases in human beings. The Chalcone-based nanoparticle, Trans-3-(9-Anthryl)-1-phenylprop-2-en-1-one (APPONPs) exhibits fluorescence

enhancement in the presence of Al^{3+} [7]. The variation in glutathione level may be responsible for several diseases, a pyrene chalcone derivative, 1-(2-hydroxyphenyl)-3-(1-pyrenyl)-2-propen-1-one, exhibits blue fluorescence enhancement for glutathione in methanol-water solution [8]. Non-linear optical properties of chalcone derivatives can be exploited in designing photonic devices which have wide applications in optical telecommunication, optical computing, and optical switching [9].

Similar to chalcone derivatives, nanoparticles are preferred in electronics, non-linear optics, energy, and catalysis [10][11]. The organic molecules exhibit fluorescence enhancement in the presence of Au NPs and the efficiency of dye-sensitized solar cells is increased in the presence of Au NPs [12][13]. Titanium dioxide (TiO_2) nanoparticles are the most preferred semiconductor NPs compared to other NPs because of their stability and low cost. They have wide applications in photo-electrochemical devices such as solar cells, biosensors, chemical sensors, biodiesel production, and in gas sensors. The TiO_2 NPs increase the therapeutic efficiency in drug delivery. Titanium dioxide is an n-type semiconductor with a wide energy band gap of 3.23 eV. The anatase phase of TiO_2 is preferred in dye-sensitized solar cells because of its high electron mobility [12-16]. The fluorescence enhancement property of polyethylene glycol-modified titanium dioxide nanoparticles is used in the diagnosis of cancer tissue [15].

Zinc oxide (ZnO) nanoparticle is also an n-type semiconductor with a wide band gap of 3.37 eV and a binding energy of 60 MeV. ZnO NPs are used in the design of LASER, as a photocatalyst, in sensors, and also in solar cells. Chalcone doped with ZnO NP is found to be useful in optoelectronic devices [16]. ZnO NPs are highly fluorescent and are applied in cancer cell imaging and photodynamic therapy [17]. The nano crystalline ZnO enhances the fluorescence intensity of the organic compound imidazole hence, this imidazole acts as a chemosensor for Zn^{2+} ions [18].

From the literature, it is confirmed that chalcone derivatives, TiO_2 and ZnO nanoparticles are exploited in optoelectronic and photonic devices because of their interesting non-linear optical properties hence in the present investigation, chalcone derivatives, 4-phenylbut-3-en-2-one (SC2), (E)-3-(4-hydroxyphenyl)-1-phenylprop-2-en-1-one (SC3) and 3-(2-hydroxyphenyl)-1-phenylprop-2-en-1-one (SC4) were chosen to study their optical properties in the presence of semiconductor nanoparticles, TiO_2 and ZnO using various spectroscopic methods. Theoretical DFT computations were carried out using B3LYP level, 6-311G basis set in Gaussian 09W.

2. MATERIALS AND METHODS

The chalcone derivatives, 4-phenylbut-3-en-2-one (SC2), (E)-3-(4-hydroxyphenyl)-1-phenylprop-2-en-1-one (SC3) [4hydroxychalcone], and 3-(2-hydroxyphenyl)-1-phenylprop-2-en-1-one (SC4) [2hydroxychalcone] were synthesized in the Department of Chemistry, Karnatak Science College, Dharwad. HPLC grade solvents dichloromethane, acetonitrile, and dimethyl sulfoxide were purchased from Nice Chemicals (P) Kochi, Kerala. Semiconductor nanoparticles (NPs), TiO2, and ZnO were purchased from Sigma Aldrich. All these solvents and NPs were used without any further purification. For absorption and fluorescence studies, the concentration of chalcone derivatives was fixed at 1×10-5 M. The absorption spectra of chalcone derivatives without and with the increasing concentration of the above mentioned NPs were recorded using the UV–Visible absorption spectrophotometer model: JASCO-V-670. The fluorescence spectra of samples were recorded using the spectrofluorometer model: Hitachi F-7000. The spectrofluorometer has a 150W Xenon lamp. Excitation and emission slit widths were maintained at 5 nm. The quartz cell of 1 cm width was used for recording absorption and fluorescence. The fluorescence intensities of these chalcone derivatives were recorded by exciting the chalcone derivatives at their respective absorption maxima. To understand the nature of the interaction between chalcone derivatives and the NPs [19], FT-IR spectra of chalcone derivatives, and NPs were recorded using the FT-IR spectrometer model: Nicolet 6700 FT-IR. Chalcone derivatives were synthesized according to the following method: Initially, a solution of ketone (10 mM) and aldehyde (10 mM) was prepared, stirred for 10 minutes, and BF2. OEt2 (2.5 mM) was gradually added at room temperature. Dry dioxane (3mL) was used as a solvent. The solution was stirred for 120 min at room temperature, subsequently washed with acidified water (2 mL), and the organic phase was extracted with ethyl acetate. The organic phase obtained was dried over anhydrous Na2SO4 and concentrated under reduced pressure. The chosen chalcone was purified by chromatography. The structures of chalcone derivatives SC2, SC3, and SC4 are shown in Fig. 1(i), (ii), and (iii) respectively.

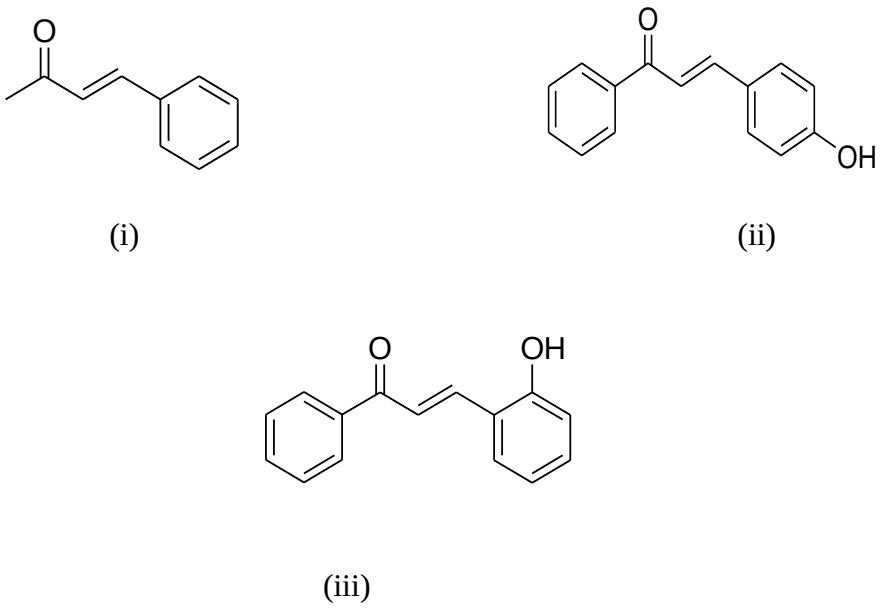

(i) (ii)

(iii)

Fig.1. Structure of chalcone derivatives (i) 4-phenylbut-3-en-2-one (SC2) (ii) (E)-3-(4-hydroxyphenyl)-1-phenylprop-2-en-1-one (SC3) (iii) 3-(2-hydroxyphenyl)-1-phenylprop-2-en-1-one (SC4)

3. RESULTS AND DISCUSSION

3.1 Analysis of UV-VIS absorption Spectra

The absorption spectra of chalcone derivatives, SC2 and SC4 were recorded separately at room temperature without and with an increasing concentration of TiO_2 and ZnO NPs in acetonitrile (MeCN) and dichloromethane (DCM) solvents. Whereas the absorption spectra of SC3 alone and with the increasing concentration of the above- mentioned NPs were recorded in acetonitrile and dimethyl sulfoxide (DMSO) solvents because SC3 is not soluble in DCM. Fig. 2 depicts the absorption spectra of a chalcone derivative, SC2, without and with increasing concentrations of TiO_2 NPs in acetonitrile. The absorption spectra of SC3 without and with the increasing concentrations of ZnO NPs in acetonitrile are shown in Fig. 3.The absorption maximum of SC2 is at 275 nm and that of SC3 is at 337 nm. The Chalcone derivative, SC4, has two absorption maxima, one at 298nm and the other at 408nm. The concentration of the NPs for the absorption measurements varied from 0.33 mM to 1.65 mM. It is observed from the absorption spectra that the absorption intensity increases with the increasing concentration of NPs, but there is no shift in the absorption peak with the increasing concentration of NPs Hence, the ground state complex is not formed between chalcone derivative and NP [20]. To understand the stoichiometry of nonbonding interactions between chalcone derivative and NP, the association constant can be calculated using the Benesi-Hildebrand equation Eq. (1)[21][22][23].

$$\frac{C}{\Delta a} = \frac{1}{\Delta \varepsilon} + \frac{1}{\Delta \varepsilon K_a [Q]} \quad (1)$$

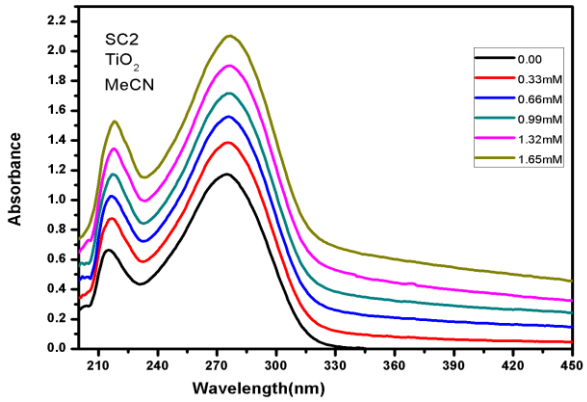

Fig.2 Absorption Spectra of chalcone derivative SC2 in the absence and with the increasing concentrations of TiO_2 NPs in acetonitrile (MeCN)

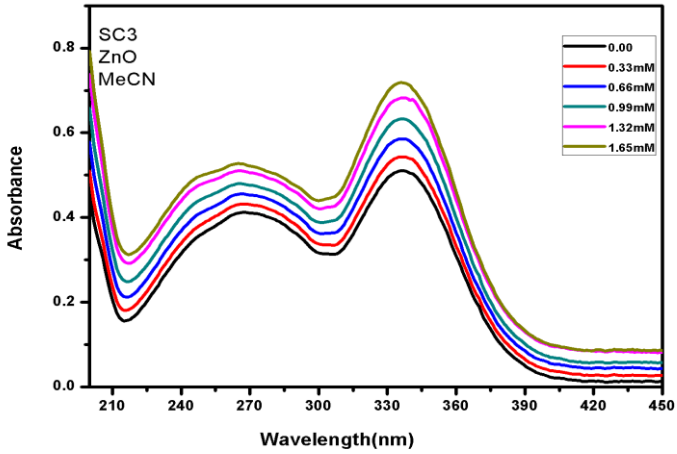

Fig.3 Absorption Spectra of chalcone derivative SC3 in the absence and with the increasing concentrations of ZnO NPs in acetonitrile (MeCN)

Here, C is the concentration of the chalcone derivative, Δa is the difference in the absorbance of the chalcone derivative in the absence and the presence of NPs at the absorption maxima. $\Delta\varepsilon$ is a change in the molar extinction coefficient, K_a is the association constant, and [Q] is the concentration of the NPs. Fig. 4(i)-(iii) show the plots of $C/\Delta a$ against 1/ [TiO_2] for the chalcone derivatives SC2, SC3, and SC4, where [TiO_2] is the concentration of TiO_2 NPs. The plots of $C/\Delta a$ versus 1/ZnO] for chalcone derivatives and ZnO NPs are shown in Fig. 5(i)-(iii). The association constant K_a is calculated using the intercept and slope of the Benesi-Hildebrand plot for all the above-mentioned chalcone derivatives and NPs. The values of the association constant for these chalcone derivative-NPs systems are shown in Table 1. The stoichiometric interaction is 1:1 between SC2 and NPs in both solvents. 1:2 interactions are observed for SC3-NPs, except in acetonitrile in the presence of TiO_2 NPs. The type of interaction is 1:1 for SC4, except in DCM solvent in the presence of ZnO NPs. 1:2 interactions are observed when Benesi-Hildebrand plots have negative intercepts and the plot of $C/\Delta a$ versus $1/[Q]^2$ is linear with the positive intercept for SC3-TiO_2 in DMSO and for SC3-ZnO in acetonitrile and DMSO and for SC4-ZnO in DCM solvent [21]. From the analysis of Benesi-Hildebrand plots, it is confirmed that there is strong interaction between chalcone derivative and nanoparticle. Gibb's free energy change ΔG for the reaction is calculated at room temperature (300K) using Eq. (2). Where K_a is the association constant, T is absolute temperature and R is gas constant. The values of ΔG are shown in Table. 1. The negative values of ΔG indicate that the process is spontaneous [21].

$$\Delta G = -RT \ln K_a \quad (2)$$

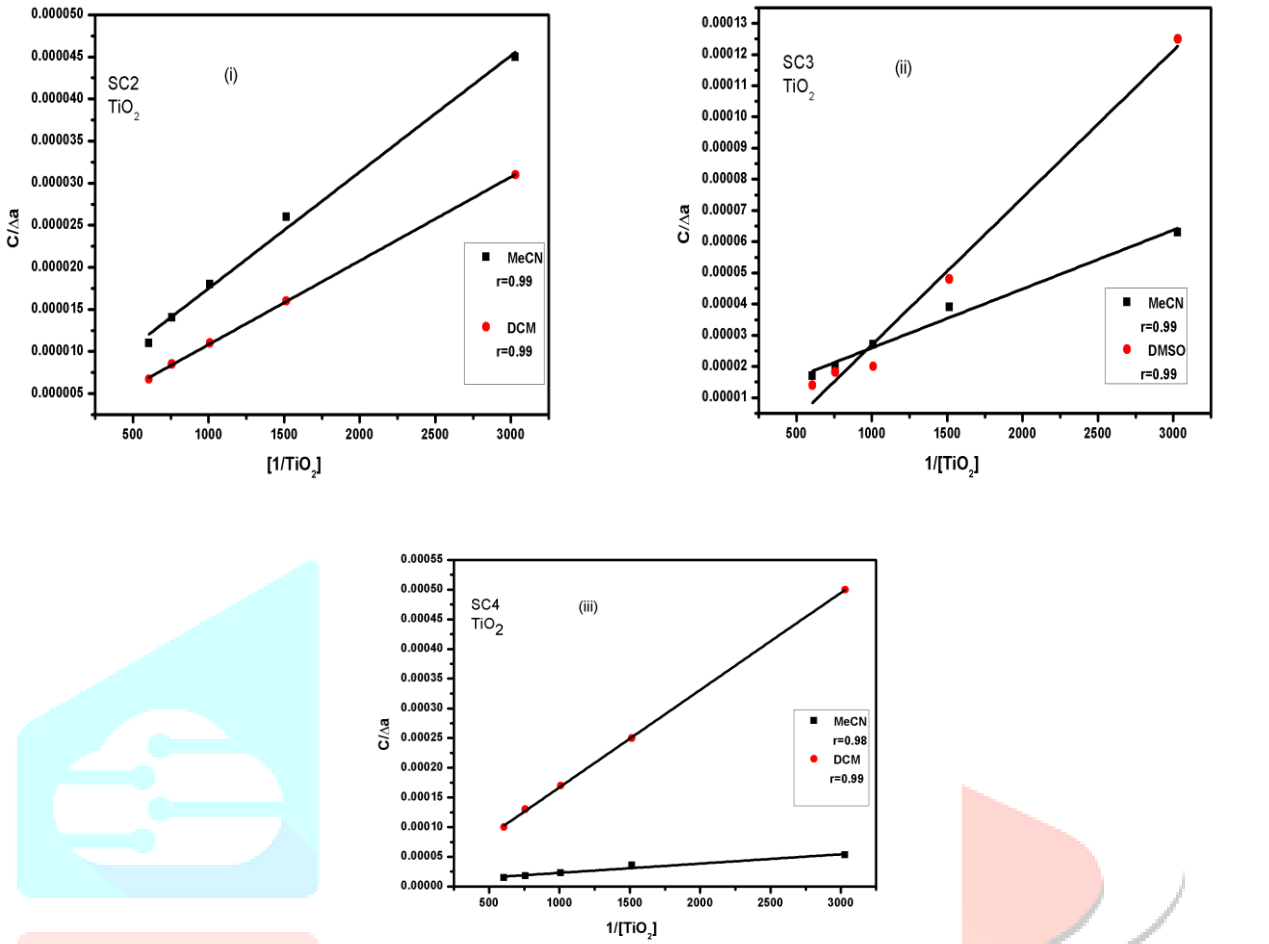

Fig.4 (i)-(iii) The Benesi-Hildebrand plot [C/Δa against 1/[TiO_2]] of chalcone derivatives SC2, SC3, and SC4 with TiO_2 NPs in acetonitrile (MeCN), dimethyl sulfoxide (DMSO), and dichloromethane (DCM) solvents

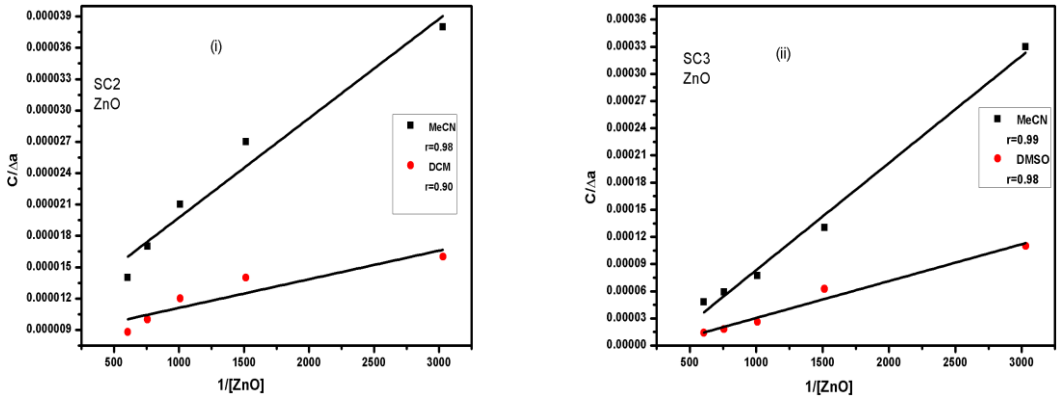

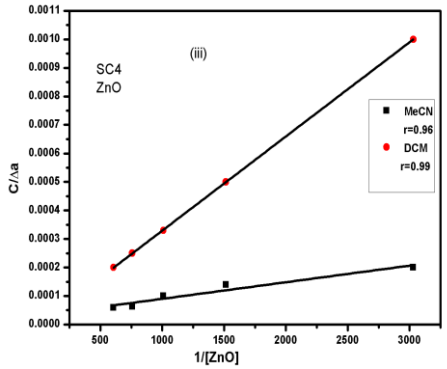

Fig.5 (i)-(iii) The Benesi-Hildebrand plot [C/Δa against 1/[ZnO]] of chalcone derivatives SC2, SC3, and SC4 with ZnO NPs in acetonitrile (MeCN), dimethyl sulfoxide (DMSO), and dichloromethane (DCM) solvents

Table. 1. The values of association constant K_a determined from Benesi-Hildebrand plots using absorption data and the values of free energy change ΔG

Chalcone Derivative	Nanoparticle	Solvent	Association constant K_a M^{-1}	Stoichiometric ratio	ΔG kJ mol^{-1}
SC2	TiO_2	MeCN	264.64	1:1	-13.91
		DCM	85.98	1:1	-11.11
	ZnO	MeCN	1078.64	1:1	-17.42
		DCM	3054.74	1:1	-20.01
SC3	TiO_2	MeCN	373.47	1:1	-14.77
		DMSO	427.97	1:2	-15.11
	ZnO	MeCN	295.43	1:2	-14.19
		DMSO	252.31	1:2	-13.79
SC4	TiO_2	MeCN	471.15	1:1	-15.35
		DCM	19.69	1:1	-7.43
	ZnO	MeCN	547.25	1:1	-15.73
		DCM	3.36	1:2	-3.02

3.2 Analysis of FT-IR spectra

The absorption spectra of chalcone derivatives in the presence of NPs indicate that there is no ground state complex formation, but the association constant determined from the Benesi-Hildebrand plot shows that there is strong interaction between chalcone derivative and NPs. Since the UV-VIS absorption study was not enough to understand the nature of bonding between chalcone derivative and NPs, FT-IR spectra of chalcone derivatives and chalcone derivatives in the presence of NPs were recorded. Fig. 6 (i)-(iii) shows the FT-IR spectra of SC2, SC2-TiO_2, and SC2-ZnO respectively. C=O stretching frequency for SC2 appears at 1712.69 cm^{-1} (Fig. 6(i)) and in the presence of TiO_2 NPs, C=O stretching frequency shifts to 1710.09 cm^{-1}, shown in Fig. 6(ii) and C=O stretching frequency shifts to 1711.56 cm^{-1} in the presence of ZnO, as shown in Fig.6 (iii). The decrease in C=O stretching is due to the coordination of NPs with the C=O group. The C=O stretching for SC3 appears at 1649.95 cm^{-1} and for SC4 at 1634.62 cm^{-1}. The significant shifts in C=O stretching frequency were not observed for SC3 and SC4 in the presence of TiO_2 and ZnO NPs because of the coordination of metal oxides with the OH group and N with the C=O group.

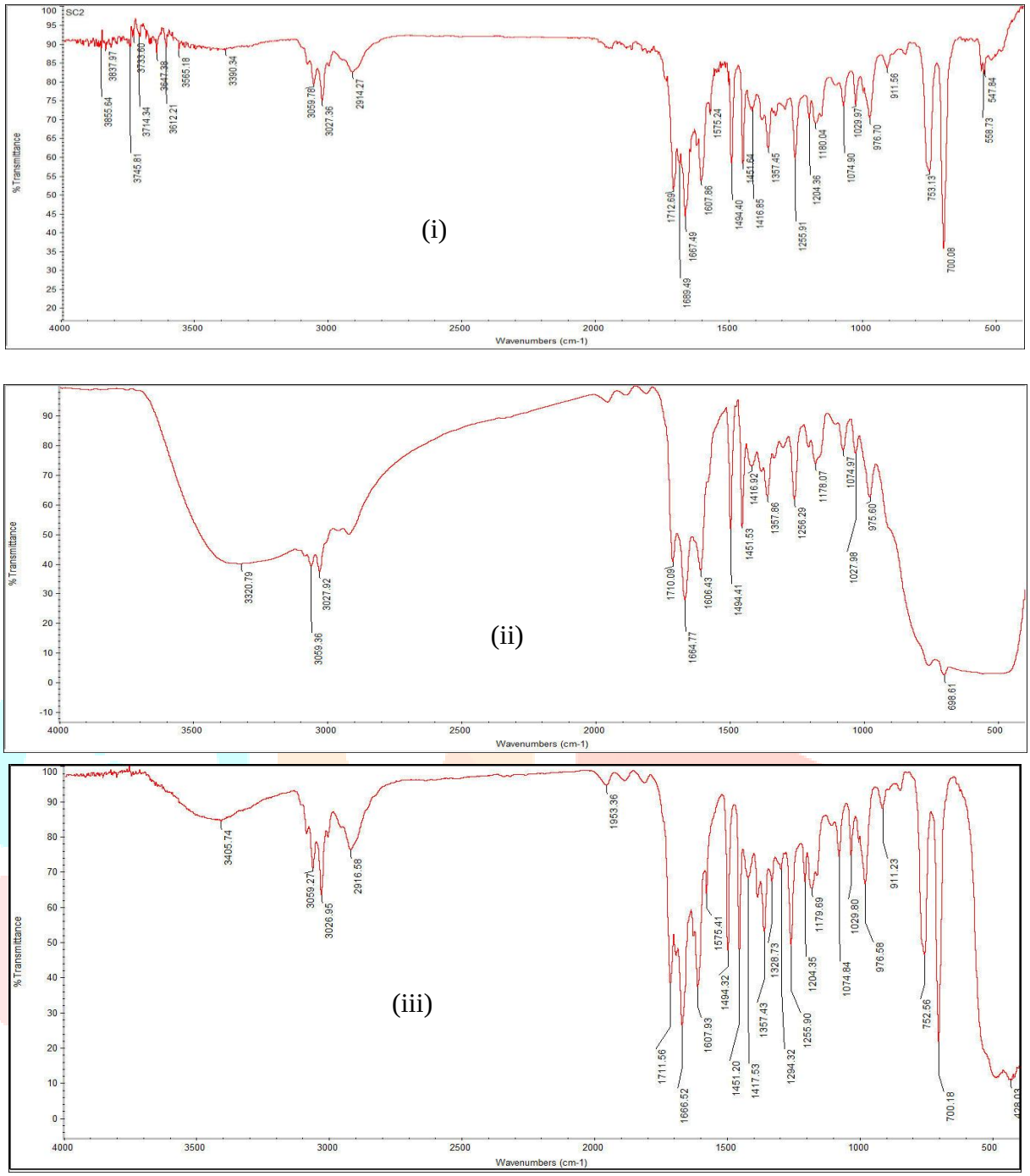

Fig.6 (i) FT-IR Spectra of Chalcone derivative SC2 (ii) SC2-TiO_2, (iii) and SC2-ZnO NPs

3.3 Analysis of Fluorescence Spectra

The fluorescence spectra of chalcone derivatives, SC2 and SC4 in the absence and with the increasing concentration of TiO_2 and ZnO NPs were recorded separately in acetonitrile and DCM solvents, whereas the fluorescence spectra of SC3 in the absence and with the increasing concentration of TiO_2 and ZnO NPs were measured in acetonitrile and DMSO solvents by varying the concentration of the NPs from 0.33 mM to 1.98mM. The fluorescence maximum of SC2 appears at 409nm. Hence, the large Stokes shift of 134nm is observed in the case of SC2 [6]. SC2 exhibits fluorescence enhancement with the addition of TiO_2 and ZnO NPs. The fluorescence maximum of chalcone derivative SC3 appears at 400 nm in acetonitrile and 426 nm in DMSO. Fluorescence enhancement is observed for SC3 with the increasing concentration of TiO_2 and ZnO NPs. The fluorescence of chalcone derivative SC4 has a double peak, one at 363nm and the other at 470nm. The fluorescence intensity of SC4, corresponding to 363nm, decreases with the increasing concentration of NPs only in acetonitrile solvent, but in DCM solvent, such a fluorescence quenching effect is not observed. The fluorescence intensity of SC4 at 470 nm increases with the increasing concentration of NPs. The fluorescence spectra

of SC2 and SC4 with increasing concentrations of TiO_2 NP in DCM solvent are shown in Fig. 7(i)-(ii). The fluorescence spectra of chalcone derivatives SC3 and SC4 in acetonitrile solvent with increasing concentrations of ZnO NPs are shown in Fig. 8(i)-(ii).

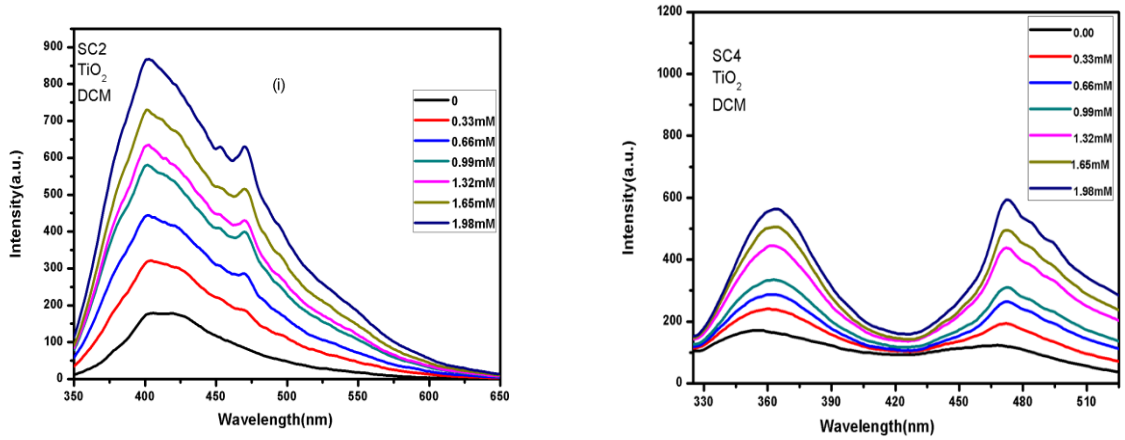

Fig.7 (i) Fluorescence spectra of chalcone derivative SC2 in dichloromethane (DCM), and (ii) SC4 in dichloromethane (DCM) in the absence and with the increasing concentration of TiO_2 NPs

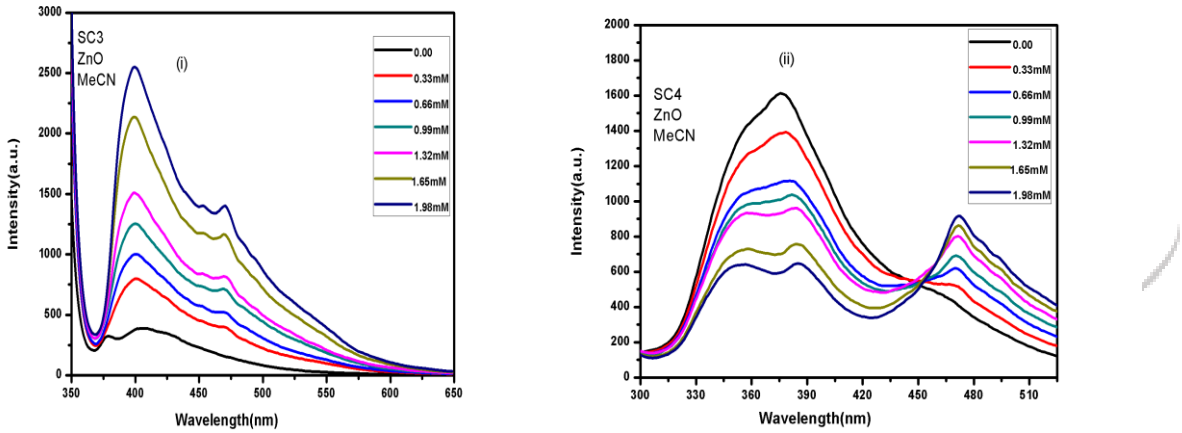

Fig.8 (i)-(ii) Fluorescence spectra of chalcone derivatives SC3 and SC4 in acetonitrile (MeCN) in the absence and with the increasing concentration of ZnO NPs

The plot of the difference in the fluorescence intensity ΔF of chalcone derivative in the absence and with the increasing concentration of TiO_2 and ZnO NPs, against the concentration of NPs for chalcone derivatives SC2, SC3 and SC4 in all the above-mentioned solvents are shown in Fig. 9(i)-(iii) and Fig. 10(i)-(iii) respectively [6][7][15][24][13]. The correlation coefficient is very close to unity in all these plots and hence it is confirmed that the fluorescence of chalcone derivative is enhanced with the increasing concentration of TiO_2 and ZnO NPs.

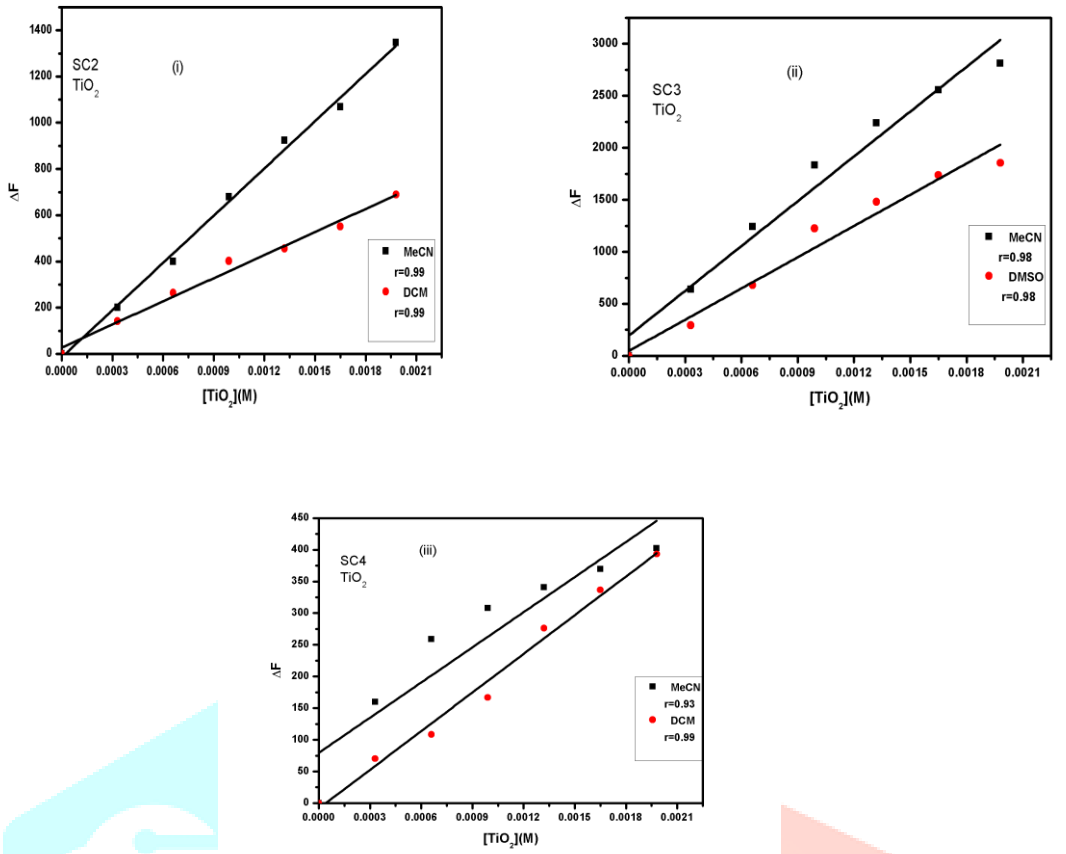

Fig.9 (i)-(iii) Fluorescence enhancement plot (ΔF against concentration of NPs[TiO_2]) of SC2, SC3 and SC4 with TiO_2 NPs in acetonitrile (MeCN), dimethyl sulfoxide (DMSO) and dichloromethane (DCM) solvents

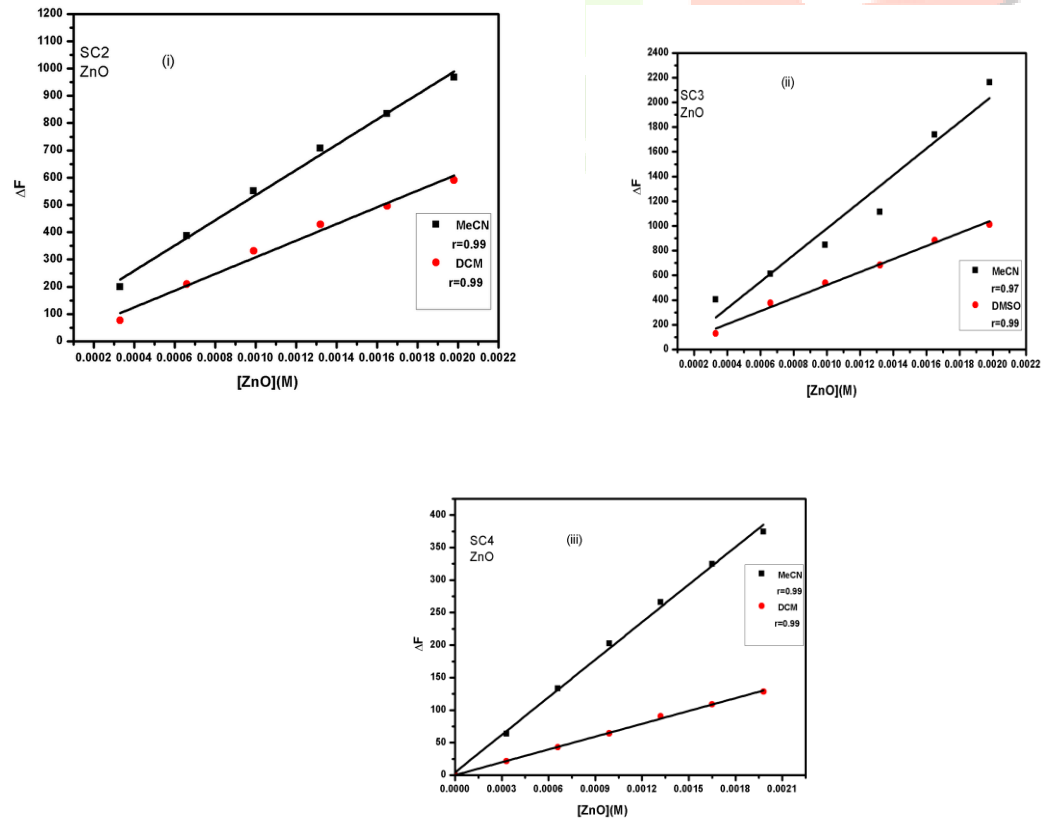

Fig.10 (i)-(iii) Fluorescence enhancement plot (ΔFagainst concentration of NPs) of SC2, SC3, and SC4 with ZnO NPs in acetonitrile (MeCN), dimethyl sulfoxide (DMSO), and dichloromethane (DCM) solvents

The association constant K is calculated using fluorescence data by plotting the graph $\frac{1}{[F-F_0]}$ against $\frac{1}{[Q]}$ according to the [25] Benesi-Hildebrand equation Eq. (3)

$$\frac{1}{[F-F_0]} = \frac{1}{[K(F_{max}-F_0)[Q]]} + \frac{1}{[F_{max}-F_0]} \quad (3)$$

Where F_0 is the fluorescence intensity of a chalcone derivative in the absence of NPs, F is the fluorescence intensity of a chalcone derivative in the presence of NPs, F_{max} is the maximum fluorescence intensity, K is the association constant, and [Q] is the concentration of the NPs. The plots $\frac{1}{[F-F_0]}$ against $\frac{1}{[TiO_2]}$ for chalcone derivative-TiO_2 NPs are shown in Fig. 11(i)-(iii) and the plots of $\frac{1}{[F-F_0]}$ against $\frac{1}{[ZnO]}$ for chalcone derivative-ZnO NPs are shown in Fig. 12(i)-(iii). The association constant K is determined from the slope and intercept of the above-mentioned plots, and the values are shown in Table.2. It is observed that the association constant K does not depend on the polarity of the solvent. The fluorescence quenching of SC4 corresponding to the peak at 363nm in acetonitrile is analyzed using Stern-Volmer plots [26][27][28][29]. The S-V plots of F_0/F against [Q] for SC4-TiO_2 and SC4-ZnO in acetonitrile solvent are shown in Fig. 13. Here, F_0 is the fluorescence intensity of SC4 in the absence of NPs and F is the fluorescence intensity in the presence of NPs. From the fluorescence study, it is confirmed that chalcone derivatives exhibit fluorescence enhancement in the presence of TiO_2 and ZnO NPs. Hence they may be used in the design of non-linear optical material.

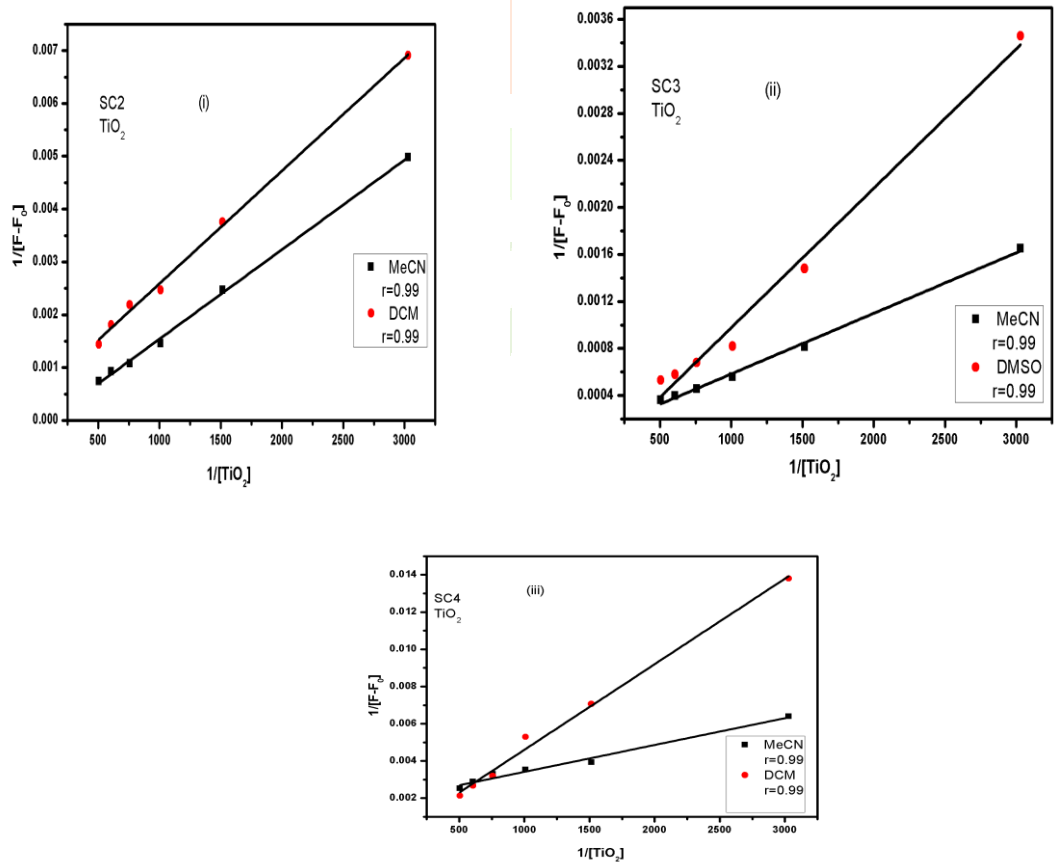

Fig.11 (i)-(iii) The plot of 1/ [F-F_0] against 1/ [TiO_2] for SC2, SC3 and SC4 in the presence of TiO_2 NPs in acetonitrile (MeCN), dimethyl sulfoxide (DMSO), and dichloromethane (DCM) solvents

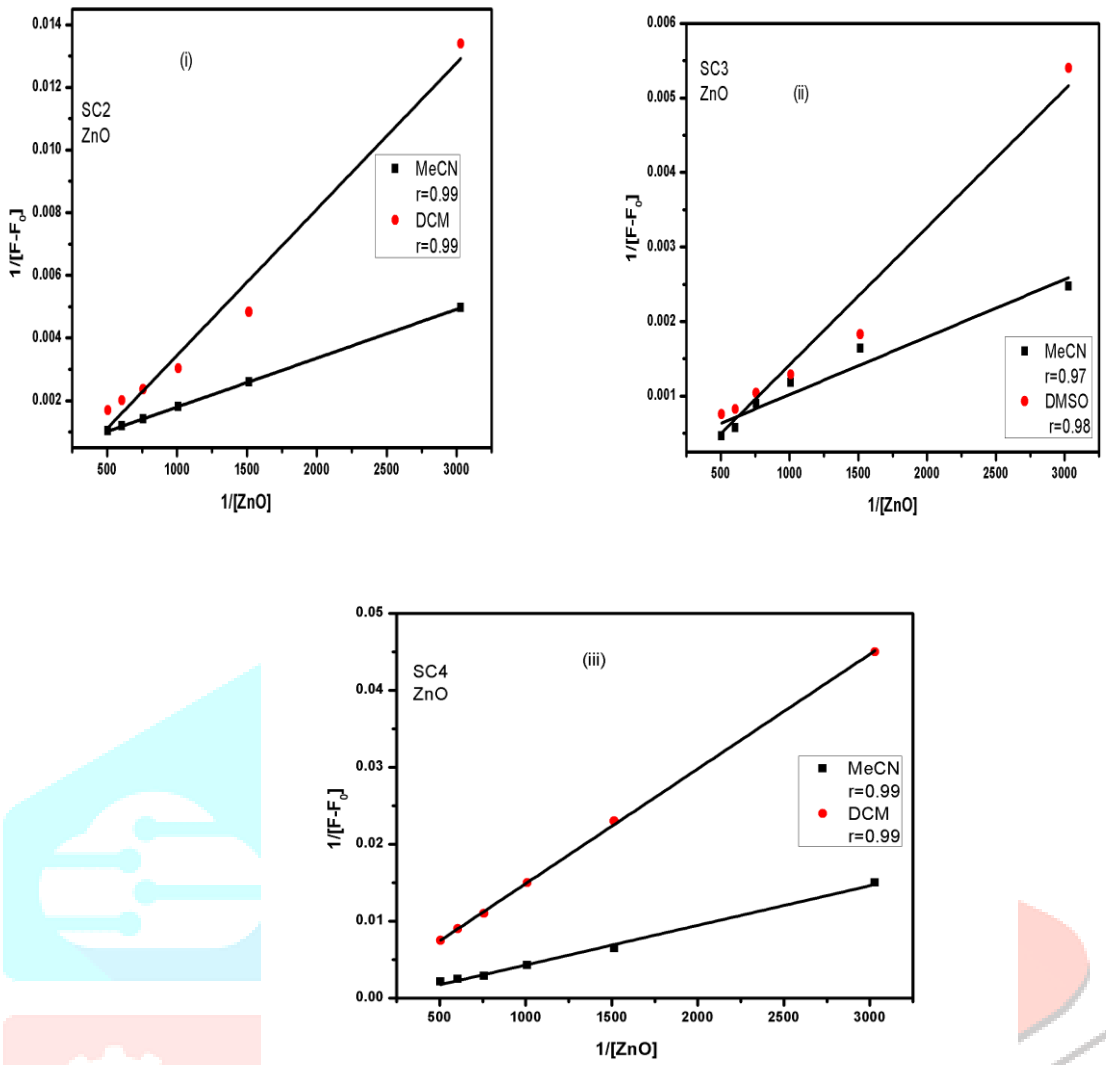

Fig.12 (i)-(iii) The plot of 1/ [F-F_0] against 1/[ZnO] for SC2, SC3 and SC4 in the presence of ZnO NPs in acetonitrile (MeCN), dimethyl sulfoxide (DMSO) and dichloromethane (DCM) solvents.

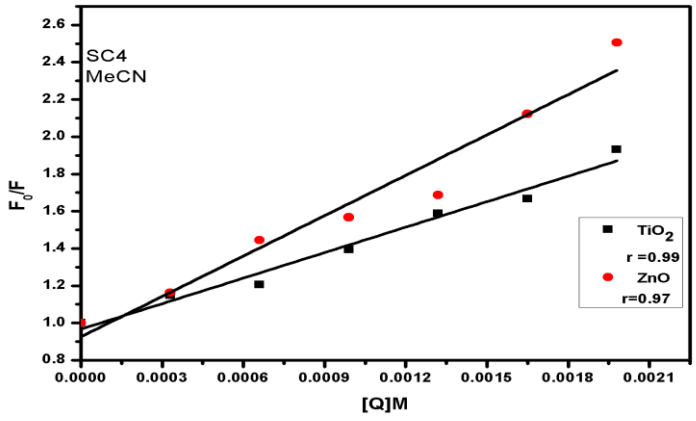

Fig.13 Stern-Volmer plot F_0/F against concentration [Q] for SC4-TiO_2 and SC4-ZnO NPs in acetonitrile

Table. 2. The values of association constant K determined from the fluorescence data

Chalcone Derivative	Nanoparticle	Solvent	Association constant K M^{-1}
SC2	TiO_2	MeCN	437.74
		DCM	674.47
	ZnO	MeCN	662.18
		DCM	361.88
SC3	TiO_2	MeCN	696.84
		DMSO	454.47
	ZnO	MeCN	598.97
		DMSO	408.77
SC4	TiO_2	MeCN	602.44
		DCM	463.88
	ZnO	MeCN	143.53
		DCM	503.02

3.4. Quantum Chemical Calculations

3.4.1. Frontier molecular orbitals

The Frontier molecular orbitals such as highest occupied molecular orbit HOMO and lowest unoccupied molecular orbit LUMO were used to determine the optical and electronic property, and chemical reactivity of the molecule. The HOMO value gives electron donating ability and LUMO gives electron accepting ability [32]. The shape of a molecule determines its physical and chemical properties. The geometry optimization and energy minimization of the molecules SC2 SC3 and SC4 were achieved using DFT, B3LYP level, 6-311G basis set in Gaussian 09W. The optimized molecular geometries and the optimized ground state molecular structures showing the dipole moment vectors of SC2, SC3, and SC4 are shown in Fig. 14. The electronic structures and electron donor/acceptor capabilities of the molecules were estimated from frontier molecular orbitals, HOMO, LUMO (Fig. 15). The theoretical ground state dipole moment, E_{HOMO}, E_{LUMO}, and energy gap ΔE in gas and solvent phases were computed using B3LYP/6-311G (d)-IEF-PCM solvation model and are shown in Table 3a, 3b and 3c respectively. It is observed that the energy gap values estimated in the gas phase and solvent phases are very close to each other. The energy gap of SC3 and SC4 is small compared to SC2, hence SC3 and SC4 are more chemically reactive, soft, and polarizable compared to SC2 [9][33][34][35]. The energy band gap values estimated from the intersection of normalized absorption and fluorescence spectra E_g^{Opt} using the relation Eq. (4) [20] are shown in Table 3a.

$$E_g^{opt} = \frac{1240}{\lambda_{onset}} \quad (4)$$

3.4.2. Global chemical reactivity descriptor (GCRD) parameters

The energy gap obtained from HOMO and LUMO values decide the chemical reactivity and polarizability of the molecule. Global chemical reactivity descriptor (GCRD) parameters can be determined from E_{HOMO} and E_{LUMO} values. The GCRD parameters are chemical hardness, $\eta = \frac{(IP - EA)}{2}$, electronegativity $\chi = \frac{(IP + EA)}{2}$, chemical potential μ= -χ, chemical softness $S = \frac{1}{2\eta}$ and electrophilicity index $\omega = \frac{\mu^2}{2\eta}$. Where $-E_{HOMO}$ = Ionization Potential (IP) and $-E_{LUMO}$ = electron affinity (EA). The GCRD parameters of SC2, SC3 and SC4 are shown in Table.4. The values of chemical hardness and chemical potentials of these molecules indicate that they are stable. The charge-transferring capacity of a molecule is determined by chemical hardness. The value of electronegativity represents the ability of the molecule to attract electrons. The global softness indicates the capacity of the molecule to receive the electrons. The value of electrophilicity index ω for all the above-mentioned organic molecules is very close to 2 hence these molecules are electrophiles. The magnitudes of GCRD parameters such as hardness, negative value of chemical potential, softness and electrophilicity index

indicate that SC2, SC3 and SC4 are stable and hence may be useful in designing non-linear optical materials [3][32][33][36][37].

3.4.3. Molecular electrostatic potential (MESP) plots

Molecular electrostatic potential (MESP) plots are constructed for SC2, SC3, and SC4 using DFT-B3LYP/6- 311G (d) model and are shown in Fig. 16. In MESP plots, red region indicates negative (nucleophilic) and blue region indicates positive (electrophilic) locations on the molecule. In all the three above-mentioned molecules, carbonyl group is moderately red indicating negative nucleophilic region [38].

3.5 Electrochemical Analysis

The Cyclic Voltammogram of chalcone derivatives, SC2, SC3, and SC4 were recorded in acetonitrile solvent with TBAPF6 as a supporting electrolyte and are shown in Fig.17. The oxidation potential values of SC2, SC3, and SC4 were determined from the CV plots and the HOMO-LUMO energy levels were calculated from the following equations Eq.(5) and Eq.(6) [20][39][40]

$$E_{HOMO} = -E_{OX}^{Onset} - 4.44 \quad (5)$$

$$E_{LUMO} = E_{HOMO} + E_{g}^{opt} \quad (6)$$

The values of E_{HOMO}, E_{LUMO} and energy gap ΔE are shown in Table 5. E_{HOMO}, E_{LUMO} and energy gap ΔE values determined from the Cyclic Voltammogram are very close to the values estimated from the DFT computation.

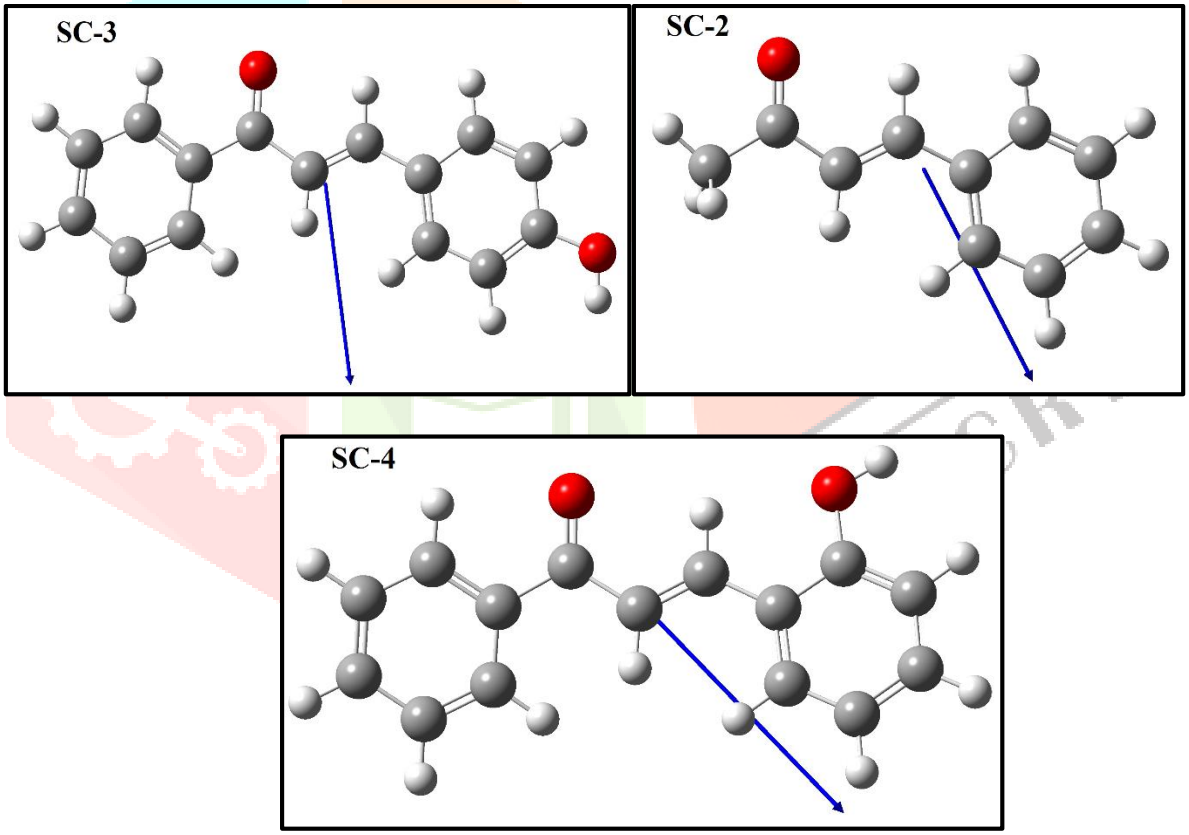

Fig. 14. Optimized molecular geometry of SC2, SC3, and SC4

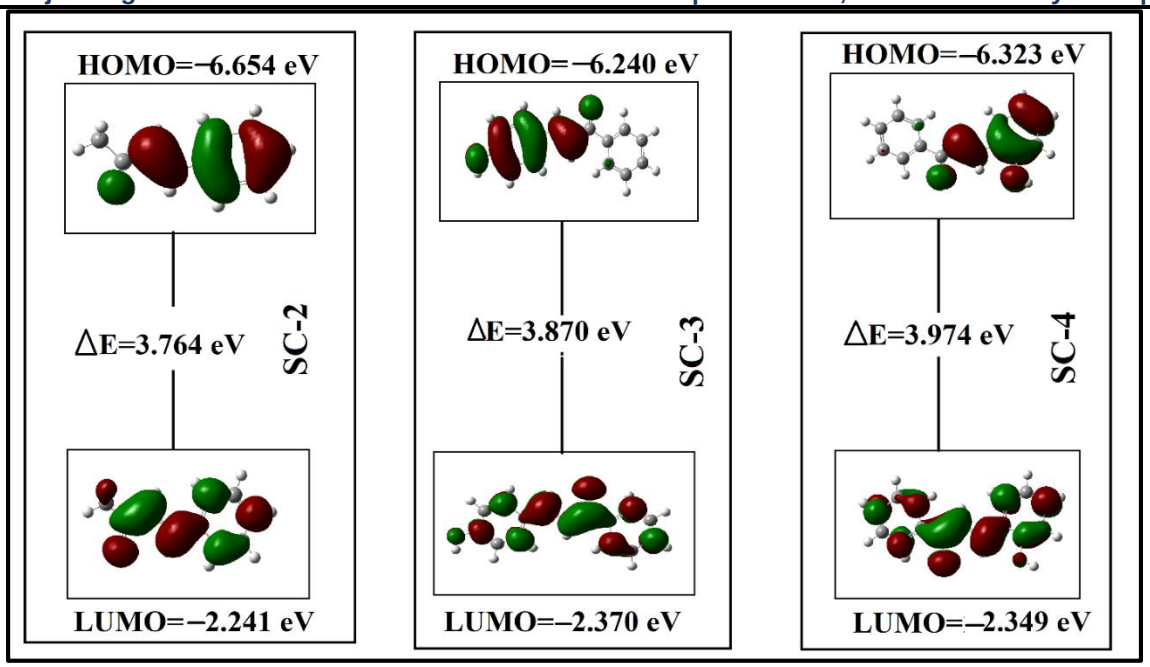

Fig. 15 3D plots of HOMO-LUMO with energy levels of SC2, SC3 and SC4

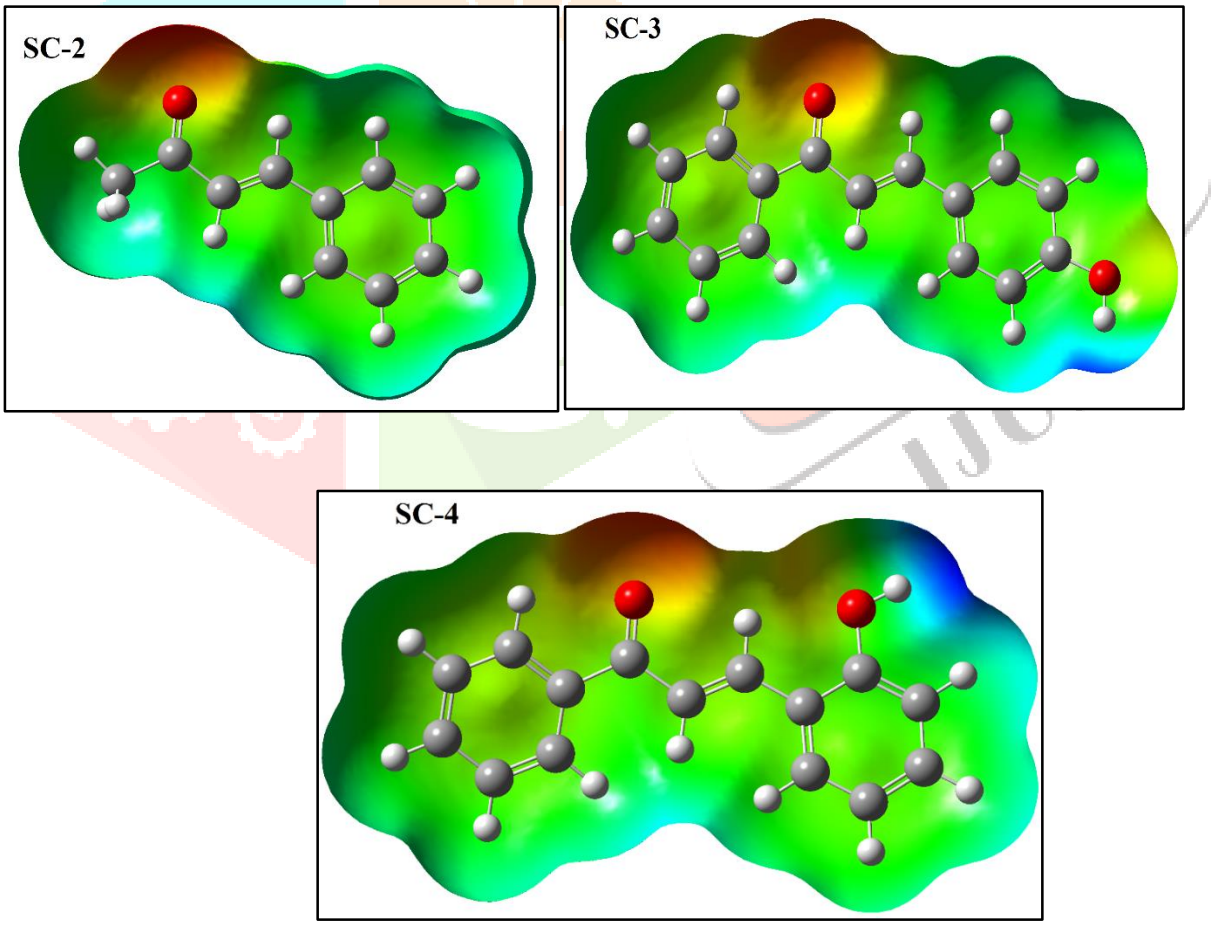

Fig. 16 Molecular Electrostatic Potential 3D plots of SC2, SC3, and SC4

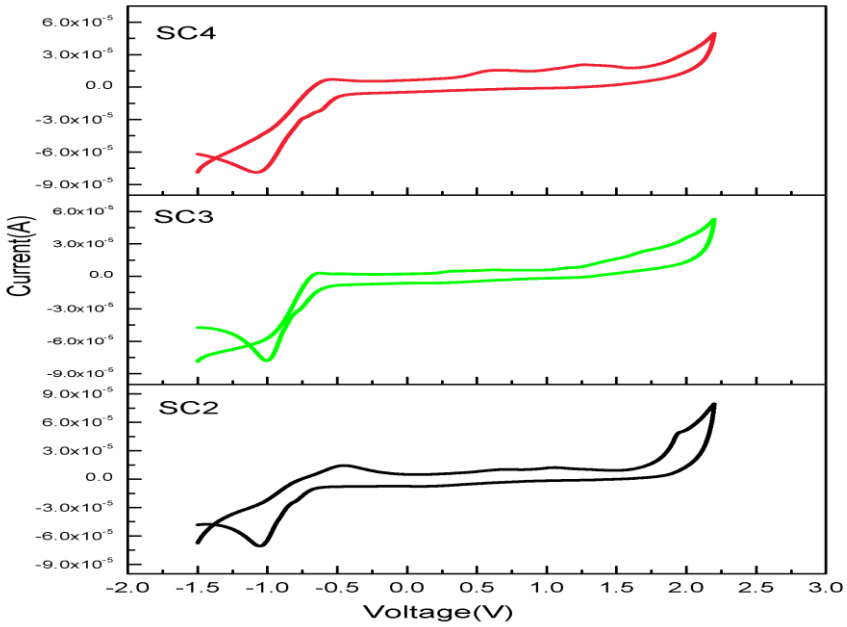

Fig. 17 Cyclic Voltammogram of SC2, SC3, and SC4 in acetonitrile

Table. 3a The values of Ground state dipole moment, molecular orbital energies (E_{HOMO}, E_{LUMO}) and energy gap (ΔE) of SC2, SC3, and SC4 in gas phase and the value of energy gap E_g^{Opt} obtained from the intersection of normalized absorption and fluorescence spectra

Molecule	Ground state dipole moment in debye	E_{HOMO} (eV)	E_{LUMO} (eV)	ΔE^a(eV)	E_g^{Opt} (eV)
SC2	3.764	-6.654	-2.241	4.413	3.800
SC3	4.226	-6.240	-2.370	3.870	3.420
SC4	4.235	-6.323	-2.349	3.974	3.580

Table-3b The values of Ground state dipole moment of SC2, SC3 and SC4 in different solvents

Solvent	Ground state dipole moment (μ_g) in debye		
	SC-2	SC-3	SC-4
Acetonitrile	4.989	6.821	5.958
DMSO		4.178	
DCM	4.817		5.982

Table-3c The values of molecular orbital energies (E_{HOMO}, E_{LUMO}) and energy gap (ΔE) of SC2, SC3 and SC4 in different solvents

Solvent	SC2			SC3			SC4		
	HOMO (eV)	LUMO (eV)	ΔE (eV)	HOMO (eV)	LUMO (eV)	ΔE (eV)	HOMO (eV)	LUMO (eV)	ΔE (eV)
Acetonitrile	-6.692	-2.363	4.328	-6.279	-2.580	3.698	-6.419	-2.637	3.782
DMSO				-6.282	-2.581	3.701			
DCM	-6.692	-2.363	4.339				-6.421	-2.641	3.779

Table. 4. The values of Global Chemical Reactivity Descriptor (GCRD) Parameters

GCRD Parameters of chalcone derivatives	SC2	SC3	SC4
Ionization potential- IP (eV)	6.654	6.240	6.323
Electron affinity- EA (eV)	2.241	2.370	2.349
Electro negativity- χ (eV)	4.447	4.305	4.336
Chemical potential- μ (eV)	-4.447	-4.305	-4.336
Chemical hardness- η (eV)	2.206	1.935	1.987
Chemical softness- S $(eV)^{-1}$	0.226	0.258	0.251
Electrophilicity- ω (eV)	2.015	2.224	2.180

Table. 5. The values of HOMO-LUMO and Energy Gap ΔE obtained from the Cyclic Voltammogram

Chalcone Derivative	HOMO	LUMO	ΔE eV
SC2	-4.91	-1.13	3.78
SC3	-5.47	-2.05	3.42
SC4	-4.86	-0.924	3.94

Conclusion:

From the present investigation, the following conclusions can be drawn:

- Benesi-Hildebrand plot obtained from the UV-VIS absorption data indicates the strong interaction between chalcone derivative and semiconductor nanoparticles.
- All three chalcone derivatives, SC2, SC3 and SC4, exhibit fluorescence enhancement in the presence of TiO_2 and ZnO NPs. The association constant determined from the reciprocal plot of fluorescence data also confirms the strong interaction between chalcone derivatives and semiconductor nanoparticles.
- According to the FT-IR study, a decrease in C=O stretching frequency of SC2 indicates coordination of NPs with the C=O group.
- Chalcone derivative SC4 shows fluorescence quenching at 363nm and fluorescence enhancement at 470 nm in the presence of TiO_2 and ZnO nanoparticles in the acetonitrile solvent.
- According to the DFT computation, Energy gap values are same in the gas phase and also in different solvents for all three chalcone derivatives. SC3 and SC4 are more chemically reactive, soft, and polarizable because they have a small energy gap compared to SC2.
- The energy gap values determined from the intersection of normalized absorption and fluorescence spectra are very close to the values obtained from the cyclic voltammetric studies.
- The global chemical reactivity descriptor (GCRD) parameters obtained from the DFT study suggest that all these chalcone derivatives are electrophiles and are stable.
- The present study indicates that these chalcone derivatives have potential applications in the design of non-linear optical materials.

Acknowledgements

One of the authors, Nirupama J.M. is thankful to the authorities of Karnatak University, Dharwad, for sanctioning the Seed Grant to carry out this research and to the staff and the Director of University Scientific Instrumentation Centre (USIC), Karnatak University, Dharwad, for providing the instrumentation facility.

References:

[1] M. G. Tay, M. H. Tiong, Y. Y. Chia, S. Hui, C. Kuan, and Z. Liu, 2016 "A Way to Improve Luminescent Efficiency of Bis-Chalcone Derivatives" J. of Chem. Vol. 2016, Article ID 3608137, 8 pages https://doi.org/10.1155/2016/3608137

[2] V. Parol, V. Upadhyaya, A. N. Prabhu, N. K. Lokanath, A. Taher, and S. R. G. Naraharisetty,2020 "A long-chain based bromo and methyl substituted chalcone derivatives ; experimental and theoretical approach on nonlinear optical single crystals A long-chain based bromo and methyl substituted chalcone derivatives ; experimental and theoretical approach," Mater. Res. Express, vol. 7, no. 5, p. 55101, doi: 10.1088/2053-1591/ab8b88

[3] S. Omar, M. Shkir, M. Ajmal Khan, Z. Ahmad, and S. AlFaify, 2020 "A comprehensive study on molecular geometry, optical, HOMO-LUMO, and nonlinear properties of 1,3-diphenyl-2-propen-1-ones chalcone and its derivatives for optoelectronic applications: A computational approach," Optik (Stuttg) vol. 204, no. October 2019, p. 164172, doi: 10.1016/j.ijleo.2020.164172

[4] S. Kagatikar and D. Sunil. 2021 "Aggregation induced emission of chalcones," Chem. Pap., vol. 75, no. 12, pp. 6147–6156, doi: 10.1007/s11696-021-01793-7

[5] S. Chen, 2021 "Novel chalcone derivatives with large conjugation structures as photosensitizers for versatile photopolymerization," J. Polym. Sci. Vol.59: 578–593., doi: 10.1002/pol.20210024

[6] H. Liu, C. Guo, S. Guo, L. Wang, and D. Shi,2019 "Design and synthesis of a fluorescent probe with a large stokes shift for detecting thiophenols and its application in water samples and living cells," Molecules, vol. 24, no. 2, pp. 1–14, doi: 10.3390/molecules24020375

[7] P. G. Mahajan, D. P. Bhopate, G. B. Kolekar, and S. R. Patil.2015"A Chalcone Based Novel Fluorescent Nanoprobe for Selective Detection of Al 3 + Ion in Aqueous Medium," J.Lumin.Appl. vol. 2, no. 1, pp. 1–13, 2015, doi: 10.7726/jla.2015.1001.

[8] Xueying Yua, Kangnan Wanga, Miaomiao Xinga, Yanan Sunb , Mengyuan Lia , Yatong Suna, Duxia Caoa, Songfang Zhaoa, Zhiqiang Liuc, 2019 "Structurally regular arrangement induced fluorescence enhancement and specific recognition for glutathione of a pyrene chalcone derivative," Anal. Chim. Acta. vol. 1082, doi: 10.1016/j.aca.2019.07.052.

[9] E. Mathew, V. V. Salian, I. Hubert Joe, and B. Narayana, 2019 "Third-order nonlinear optical studies of two novel chalcone derivatives using Z-scan technique and DFT method,"Opt. Laser Technol. vol. 120, p.105697, doi: 10.1016/j.optlastec.2019.105697

[10] H. R. Deepa, H. M. S. Kumar, M. Basanagouda, and J. Thipperudrappa, 2014 "Influence of silver nanoparticles on absorption and fluorescence properties of laser dyes," Can. J. Phys. vol. 92, no. 2, pp. 163–167, doi: 10.1139/cjp-2013-0133.

[11] P. Prosposito, L. Burratti, I. Venditti, 2020 "Silver Nanoparticles as Colorimetric Sensors for Water Pollutants," Chemosensors. Vol.8,26:doi:10.3390/chemosensors8020026 pp. 1–29.
[12] A. A. Shah, A. A. Umar, and M. M. Salleh, 2016 "Efficient quantum capacitance enhancement in DSSC by gold nanoparticles plasmonic effect," Electrochim. Acta, vol. 195, pp. 134–142, doi: 10.1016/j.electacta.2016.02.148
[13] Cuihong Li, Xiaofeng Liu, Mingjian Yuan, Junbo Li,Yanbing Guo, Jialiang Xu, Mei Zhu, Jing Lv, Huibiao Liu, and Yuliang Li, 2007 "Unusual fluorescence enhancement of a novel carbazolyldiacetylene bound to gold nanoparticles," Langmuir. vol. 23, no. 12, pp. 6754–6760, doi: 10.1021/la070110k
[14] U. P. Raghavendra, M. Basanagouda, A. H. Sidrai, and J. Thipperudrappa, 2016 "Spectroscopic investigations on the interaction of biologically active 4-aryloxymethyl coumarins with TiO2 nanoparticles," J. Mol. Liq., vol. 222, pp. 601–608, doi: 10.1016/j.molliq.2016.07.088.
[15] K. Kanehira, Y. Yano, H. Hasumi, H. Fukuhara, and K. Inoue, 2019 "Fluorescence Enhancement E ff ect of TiO 2 Nanoparticles and Application for Photodynamic Diagnosis." Int. J. Mol. Sci. (2019), 20, 3698; doi: 103390/ijms20153698
[16] M. F. Attia and A. A. Elbadawi, 2021 "Structural and optical characteristic (MSPPP) Chalcone doped ZnO nanoparticles," J. of Materials Science: Materials in Electronics (2021) vol. 2, no. 50 ml, pp. 28–34
[17] A. Bhogalea, N. Patel, P. Sarpotdar, J. Mariamc, P.M. Dongrec, A. Miotello, D.C. Kothari 2013 " Systematic investigation on the interaction of bovine serum albumin with ZnO nanoparticles using fluorescence spectroscopy" Colloids and Surfaces B: Biointerfaces. vol. 102, pp. 257–264,
[18] J. Jayabharathi, C. Karunakaran, and V. Kalaiarasi, 2015 "Thermodynamically feasible photoelectron transfer from bioactive π-expanded imidazole luminophores to ZnO nanocrystals" New J. Chem., vol. 39, no. 3, pp. 1800–1813, 2015, doi: 10.1039/c4nj02003k.
[19] A. Kathiravan and R. Renganathan,2009 "Photosensitization of colloidal TiO2 nanoparticles with phycocyanin pigment," J. Colloid Interface Sci. vol. 335, pp. 196–202, doi: 10.1016/j.jcis.2009.03.076.
[20] L. S. Chougala, J. S. Kadadevarmath, A. A. Kamble, P. K. Bayannavar, M. S. Yatnatti, R. K. Linganagoudar, J. M. Nirupama, R. R. Kamble, Qiquan Qiao 2017 "Effect of TiO2 nanoparticles on newly synthesized phenothiazine derivative-CPTA dye and its applications as dye sensitized solar cell," J. Mol. Liq., vol. 244, pp. 97–102, doi: 10.1016/j.molliq.2017.08.120.
[21] S. K. Ghatak, D. Dey, S. Sen, and K. Sen, 2013 "Aromatic amino acids in high selectivity bismuth (III) recognition," Analyst, vol. 138, no. 8, pp. 2308–2314, 2013, doi: 10.1039/c3an36842d
[22] J. M. Nirupama, R. Melavanki, N. I. Khanapurmath, L. S. Chougala, M. V Kulkarni, and J. S. Kadadevarmath, 2021 "Influence of substituent position in aromatic diamines on coumarin derivative," J. Photochem. Photobiol. A Chem., vol. 422, p. 113560, 2022, doi: 10.1016/j.jphotochem.2021.113560.
[23] H. R. Deepa, J. Thipperudrappa, and H. M. Suresh Kumar, 2015 "A study on fluorescence quenching of a laser dye by aromatic amines in alcohols," Can. J. Phys. vol. 93, no. 4, pp. 469–474, doi: 10.1139/cjp-2014-0190.
[24] K. Rurack, 2001 "Flipping the light switch 'ON' - The design of sensor molecules that show cation-induced fluorescence enhancement with heavy and transition metal ions," Spectrochim. Acta - Part A Mol. Biomol. Spectrosc. vol. 57, no. 11, pp. 2161–2195, doi: 10.1016/S1386-1425(01)00492-9
[25] M. A. Rankin and B. D. Wagner, 2004 "Fluorescence enhancement of curcumin upon inclusion into cucurbituril," Supramol. Chem., vol. 16, no. 7, pp. 513–519, doi: 10.1080/10610270412331283583
[26] V. V. Koppal, R. M. Melavanki, R. A. Kusanur, and N. R. Patil, 2018 "Understanding fluorescence resonance energy transfer between biologically active coumarin derivative and silver nanoparticles using steady state and time resolved spectroscopic methods," J. Mol. Liq., vol. 269, pp. 381–386, doi: 10.1016/j.molliq.2018.08.077
[27] J. M. Nirupama, N. I. Khanapurmath, L. S. Chougala, M. V. Kulkarni, and J. S. Kadadevarmath, 2019 "Effect of stereo electronic factors of coumarin derivatives during their interaction with TiO2 nanoparticles," J. Mol. Liq., vol. 291, p. 111266, 2019, doi: 10.1016/j.molliq.2019.111266.
[28] N. R. Patil, R. M. Melavanki, S. B. Kapatkar, K. Chandrashekhar, H. D. Patil, and S. Umapathy,2011 "Fluorescence quenching of biologically active carboxamide by aniline and carbon tetrachloride in different solvents using Stern-Volmer plots," Spectrochim. Acta - Part A Mol. Biomol. Spectrosc. vol. 79, no. 5, pp. 1985–1991, doi: 10.1016/j.saa.2011.05.104
[29] N. M. Jagadeeshwar, N. I. Khanapurmath, L. S. Chougala, M. V. Kulkarni, and J. S. Kadadevarmath, 2021 "Role of Substituent Position in Coumarin Derivatives during their Interaction with TiO_2 Nano Particles," J. Fluoresc. vol. 31, no. 3, pp. 775–785, 2021, doi: 10.1007/s10895-021-02706-3.

[30] T. Theivasanthi and M. Alagar, 2013 "Titanium dioxide (TiO2) Nanoparticles XRD Analyses: An Insight,". http://arxiv.org/abs/1307.1091.
[31] R. Yoshii, A. Hirose, K. Tanaka, and Y. Chujo, 2014 "Boron diiminate with aggregation-induced emission and crystallization- induced emission-enhancement characteristics," Chem. - A Eur. J., vol. 20, no. 27, pp. 8320–8324, doi: 10.1002/chem.201402946.
[32] M. Krishna Priya, B. K. Revathi, V. Renuka, S. Sathya, and P. Samuel Asirvatham, 2019 "Molecular structure, spectroscopic (FT-IR, FT-Raman,13C and 1H NMR) analysis, HOMO-LUMO energies, mulliken, MEP and thermal properties of new chalcone derivative by DFT calculation," Mater. Today Proc., vol. 8, pp. 37–46, doi: 10.1016/j.matpr.2019.02.078
[33] S. R. Maidur, P. S. Patil, A. Ekbote, T. S. Chia, and C. K. Quah,2016 "Molecular structure, second- and third-order nonlinear optical properties and DFT studies of a novel non-centrosymmetric chalcone derivative: (2E)-3-(4-fluorophenyl)-1-(4-{[(1E)-(4-fluorophenyl)methylene]amino}phenyl)prop-2-en-1-one," Spectrochim. Acta - Part A Mol. Biomol. Spectrosc. vol. 184. pp. 342–354, 2017, doi: 10.1016/j.saa.2017.05.015
[34] Lohit Naik, M.S. Thippeswamy, V. Praveenkumar, G.H. Malimath, D. Ramesh, Suraj Sutar, Hemantkumar M. Savanur e , S.B. Gudennavar a , S.G. Bubbly 2023 "Solute-solvent interaction and DFT studies on bromonaphthofuran 1,3,4-oxadiazole fluorophores for optoelectronic applications" J. Mol. Graph. Model. Vol. 118, 108367
[35] V. K. Choudhary, A. K. Bhatt, D. Dash, and N. Sharma, 2019 "DFT calculations on molecular structures, HOMO–LUMO study, reactivity descriptors and spectral analyses of newly synthesized diorganotin(IV) 2-chloridophenylacetohydroxamate complexes," J. Comput. Chem., vol. 40, no. 27, pp. 2354–2363, 2019, doi: 10.1002/jcc.26012.
[36] R. G. Pearson, 2005 "Chemical hardness and density functional theory," J. Chem. Sci., Vol. 117, No. 5, pp. 369–377.
[37] P. K. Chattaraj, B. Maiti, and U. Sarkar, 2003 "Philicity: A Unified Treatment of Chemical Reactivity and Selectivity" J. Phys. Chem. A. vol. 107, 25, 4973–4975
[38] G. P. S. Mol, D. Aruldhas, and I. H. Joe, 2022 "Heliyon Chemical reactivity, molecular electrostatic potential and in-silico analysis on benzimidazole fungicide benomyl," Heliyon. vol. 8, p. e11417, doi: 10.1016/j.heliyon.2022.e11417.
[39] J.M. Nirupama, N.I. Khanapurmath, L.S. Chougala, L.A. Shastri, R.F. Bhajantri, M.V. Kulkarni, J.S. Kadadevarmath 2019 "Effect of amino anilines on the fluorescence of coumarin derivative," J. Lumin. vol. 208, pp. 164–173, doi: 10.1016/j.jlumin.2018.12.038.
[40] M. Kumbhakar, S. Nath, T. Mukherjee, and H. Pal, 2005 "Effect of micellar environment on Marcus correlation curves for photoinduced bimolecular electron transfer reactions," J. Chem. Phys. vol. 123, no. 3, doi: 10.1063/1.1953579.